Construction and Building Materials 413 (2024) 134943

Contents lists available at ScienceDirect

Construction and Building Materials

journal homepage: www.elsevier.com/locate/conbuildmat

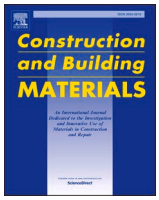

Investigation of sisal fiber incorporation on engineering properties and sustainability of lightweight aggregates produced from municipal solid waste incinerated bottom ash

Helong Song [a], Tao Liu [b,*], Florent Gauvin [a,*], H.J.H. Brouwers [a]

[a] Department of the Built Environment, Eindhoven University of Technology, P. O. Box 513, 5600 MB Eindhoven, the Netherlands
[b] DTU sustain, Department of Environmental and Resource Engineering, Technical University of Denmark, Brovej 118, 2800 Kongens Lyngby, Denmark

ARTICLE INFO

Keywords:
MSWI bottom ash
Sisal fiber
Synthesized lightweight aggregates
Strength performance
Environmental and economic assessment

ABSTRACT

The large-scale disposal of bottom ash resulting from municipal solid waste incineration poses a significant challenge in terms of effective management. While Lightweight aggregates made of municipal solid waste incinerated bottom ash, referred to as MSWI BA, show promise, their practical application is hindered by low structural strength and the presence of certain contaminants. To address this, a novel and green solution is proposed in this study, which involves utilizing sisal fibers (SF) to enhance the solidification of the synthesized aggregates. In this study, the synthesized lightweight aggregates (SLWAs) consisting of cement, different replacement levels of ground MSWI BA (60%, 70%, and 80%), and/or the cut SF were manufactured by a disc pelletizer. The influence of incorporating SF on the SLWAs was investigated across various aspects, encompassing the physical characteristics, strength performance, microscopic properties, and sustainability. The results showed that when SF was incorporated, the production efficiency of coarse SLWAs was considerably improved, especially up to a 66.5% increase with under the 70% replacement level of MSWI BA. Moreover, the surface roughness and strength were improved due to the SF addition. In the system of the CEM-MSWI BA matrix, the fiber incorporation not only accelerates the cement hydration reaction but also fills the pore generated from the swelling of metallic aluminum in MSWI BA, achieving the strength enhancement of SLWAs. More importantly, some contaminant ions including chloride, chromium, and copper from MSWI BA, could be effectively absorbed and solidified by the SF. Furthermore, the utilization of SF in SLWAs brings about great sustainability concerning greenhouse gas emissions and production costs. Consequently, incorporating SF proves to be an effective and green solution, thus promoting the practical implementation of the SLWAs.

1. Introduction

Worldwide, municipal solid waste (MSW) is generated at a rate of around 2.1 billion tonnes annually and incineration is the most common and effective treatment to reduce its mass (70–80%) and volume (around 90%) [1,2]. On the other hand, managing these incinerated residues has become a thorny problem. Municipal solid waste incinerated bottom ash (MSWI BA) is the largest residue fraction from waste-to-energy plants. In Europe, about 20 million tons of MSWI BA are produced per year [3]. However, due to low commercial value, most of the MSWI BA has to be disposed of in landfills rather than utilized in other fields. Landfilling of such enormous amounts of MSWI BA results in the pollution of groundwater and soil and even threatens human health owing to its heavy metal contents. Meanwhile, the increased landfilling tax and the EU landfill directive increase the cost of landfilling [4], Therefore, finding a new sustainable solution for utilizing MSWI BA is quite urgent.

Consequently, in the past few years, adding MSWI BA for the production of building materials has attracted more and more interest due to its phy-chemical properties and mineralogical composites [5,6]. The primary forms of MSWI BA employed in mortars/concrete were categorized in two ways: artificial aggregates [7–9] and supplementary cementitious material [10,11]. Currently, the technique of cold-bonded pelletization for aggregate production is the most commonly adopted by many researchers due to a series of advantages (low energy consumption, low cost, and low carbon footprint) [12]. Furthermore, to

* Corresponding authors.
E-mail addresses: taliu@dtu.dk (T. Liu), f.gauvin@tue.nl (F. Gauvin).

https://doi.org/10.1016/j.conbuildmat.2024.134943
Received 30 October 2023; Received in revised form 4 January 2024; Accepted 5 January 2024

maximize the utilization of MSWI BA, some scholars attempted to improve the proportion of MSWI BA in artificial aggregates. For instance, Liu et al. [13] explored different amounts (10–60% of the total solid) of the binder (cement and ground granulated blast furnace slag) to bond MSWI BA for artificial lightweight production. The results showed that 30% of the total solid reached the optimal condition considering the production efficiency and MSWI BA recycling rate. However, the building products prepared by MSWI BA were found to have low strength due to the undesirable swelling of metallic aluminum under the alkaline environment with hydrogen emission [9], and serious contaminating ions leaching (e.g., heavy metal ions, chloride, and sulfate anions). Two main drawbacks would limit its practical application in the building industry. To address them, many attempts have been made. Firstly, regarding the low strength problem, there are currently some solutions through reducing the metallic aluminum content: (1) Pre-storage under water before use [14]; (2) Wet milling pretreatment [15]; (3) Hydrothermal treatment for increased strength and reduced leaching [16]; (4) Washing with alkaline solution [17,18]; (5) Physical separation by special mechanical equipment [3]. These treatments can effectively reduce the content of metallic aluminum, contributing to strength development. On the other hand, they simultaneously bring new problems such as longer time costs, higher expenses, and more complex processes. Secondly, for the leaching problem, water washing repeatedly is a common way to treat MSWI BA to minimize the contaminating ions release [19,20]. However, this method could not effectively remove the aluminum and even caused secondary water pollution. In addition, it was reported from the literature [21] that accelerated carbonation has the potential to encapsulate heavy metal ions from MSWI BA. On the other hand, it was proven that this treatment also increases chloride and sulphate anion release [22]. It is well-known that cement can immobilize the contaminants of MSWI BA through hydration products [23,24]. However, due to the low content of cement binder used in aggregate production, the immobilization effect of contaminated ions may be insufficient. Therefore, it is necessary to add an effective solidification technique used in the contaminated ions immobilization of synthesized aggregates.

In recent years, there has been significant interest in utilizing plant fibers as potential reinforcement in composite materials for construction, owing to their impressive tensile strength and ecological benefits [25–27]. Anandaraj et al. [28] reported that applying sugarcane bagasse fibers in the concretes incorporated could effectively develop mechanical strength. Beyond construction, researchers in the field of wastewater management have exploited the distinctive hollow lumen structures and negative charges of plant fibers for the absorption of dyes and hazardous heavy metal ions [29]. However, the unique structure characteristic of plant fibers has yet to be utilized in cementitious composites. Considering the presence of contaminant ions in MSWI BA, the incorporation of plant fibers can be anticipated to immobilize these contaminant ions during the production of MSWI BA-based aggregates. Nevertheless, to the best of the authors' knowledge, no studies have analyzed the effect of plant fiber incorporation into artificial aggregates with MSWI BA.

In addition, due to the low carbon footprint characteristic of MSWI BA and carbon neutral policy, many researchers have reported the carbon emission impact of MSWI BA utilized in the building field [30–32]. For example, Shi et al. [33] analyzed the carbon emission when MSWI BA was conducted on road construction. They found that when MSWI BA was applied in a second-class highway base, CO_2 emissions could be significantly reduced. However, until now, few studies about the impact of the production of MSWI BA-based artificial aggregates on carbon emission have been reported.

Considering the above, the purpose of this study is to explore the feasibility of the MSWI BA-based aggregates incorporated with plant fibers and provide scientific insight for developing a new solidification technology from the strength properties and contaminant leaching. Sisal fiber (SF) was selected considering its rich hollow sub-fibers [34], and a cold-bonded pelletizing technique was employed in this work. A comprehensive experiment work including physical properties, mechanical strength, and microstructure characteristics of aggregates was conducted. Then the mechanisms of strength development and contaminants immobilization were also explored in depth. Finally, the impacts of MSWI BA-based synthesized aggregates on the environment and related manufacture cost evaluation were investigated.

2. Materials and methods

2.1. Materials

MSWI BA sourcing from Heros (the Netherlands) was employed in this experiment. The incineration process has been described in the previous study [35], and the chemical composition of MSWI BA is listed in Table 1. SF was supplied by Wageningen University (the Netherlands). The geometry and chemical composition of SF are given in Table 2. The cement as the binder was selected CEM I 52.5 R (ENCI, the Netherlands) in order to have a rapid hydration reaction to achieve early-period strength.

2.2. Pretreatment

In this experiment, the same batch of SF was cut twice into very fine fibers using a cutting mill (SM 100, Retsch) to ensure a homogeneous dispersion within the cement and MSWI BA particles. The raw MSWI BA from the plant was first dried in the oven at 60 °C due to some water content according to EN 933–1. The moisture content was tested at approximately 8%. The carbon emissions and fees during the drying process were also calculated into the carbon emissions and cost assessment in the subsequent section.

The particle size of raw MSWI BA is determined by the sizing method according to ASTM-C136. The maximum particle size of raw MSWI BA was no more than 5 mm. The fineness modulus (FM) of fine particles is 4.8, which means the average size is between 0.3 mm and 0.6 mm. After that, the MSWI BA was milled (Vibratory disc mill RS300, Retsch) for the powder in order to the effective and homogeneous aggregate production. Finally, the particle size distribution of milled MSWI BA and CEM I 52.5 R are also tested (Mastersizer 2000, Malvern), illustrated in Fig. 1.

2.3. Synthesized sustainable lightweight aggregate

In view that the pozzolan activity is slightly low and the hydration capacity is weak [36,37], it is necessary to add OPC to stimulate pozzolanic activity, and then the gelling and bonding effect of the chemical reaction was applied to combine MSWI BA to form synthesized lightweight aggregates (SLWAs). This principle has been also reported in the literature [38], [39]. In order to ensure that the cut sisal fibers and MSWI BA can be fully bonded by the binders, it is necessary to find a suitable water/cement ratio before manufacturing. After several trials, the liquid-solid (cement and MSWI BA) ratio was determined at about 25% on the weight of the cementitious materials. However, the slight variation in practical liquid-solid ratio was observed among groups (Table 3). This is primarily attributed to practical operational factors. Occasionally, some of the fogged water may spray on the inner wall or even out of the pelletizer, rather than all targeting the dried particle surfaces. This results in a minor loss of water loss or a minor addition of water supplementary, leading to a deviation in the calculated liquid-solid ratio. However, the practical liquid-solid ratio used to produce the aggregates should be considered as consistent.

In addition, it was found that the bonding effect of SLWAs was very loosened when the mass percentage of MSWI BA constituent occupied over 80%. Thus, the replacement proportions with MSWI BA range from 60% to 80% here. In this work, the cold bonded method was adapted to manufacture the aggregate. The size of the disc pelletizer (ERWEKA-AR 403) is specified as follows: 100 cm diameter and 15 cm high. The detailed parameters were modified based on the information from the

Table 1
XRF analysis results of MSWI BA (% by weight).

	SiO_2	CaO	Al_2O_3	Fe_2O_3	MgO	Others	LOI	Specific density
Oxides	36.5	22.7	16.3	13.7	1.3	0.7	8.8	2.1

Table 2
Geometry characteristics and chemical composition of SF.

	Geometry characteristic			Chemical composition[36]			
	Length (L, mm)	Diameter (D, μm)	L/D (%)	Cellulose (%)	Lignin (%)	Hemicellulose (%)	Extractive (%)
SF	60	200	300	67-78	8-11	10-14	2

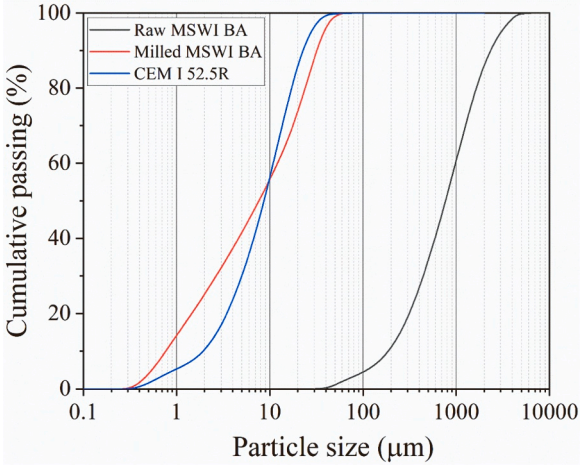

Fig. 1. Particle size distribution of Raw MSWI BA, Milled MSWI BA, and CEM I 52.5 R.

Table 3
The fraction of raw materials to synthesize green LWA.

Item		**W/C** (%)	**Fibers** (wt%)	**MSWI BA** (wt%)	**Cement** (wt%)
S1	S1-C	24.20	-	60	40
	S1-F	24.74	2		
S2	S2-C	23.66	-	70	30
	S2-F	28.62	2		
S3	S3-C	26.54	-	80	20
	S3-F	24.35	2		

Noting: (1) The unit: wt% means the weight percentage relative to the total inorganic mass (MSWI BA and cement).

literature from Tang [40], and the practical manufacturing effect. The coordination of synthesized LWA is illustrated in Table 3. The manufacturing process is presented in Fig. 2. Before manufacturing lightweights, the raw solid materials were first mixed sufficiently within a plastic bucket by shaking up and down for 3 min. Partly mixed materials (around 30% of total solid weight) were placed on the running disc at 60 rpm. The water was sprayed continuously onto the surface of dried materials. This process lasted about 15 min. After that, the running disc speed was changed to 70 rpm and then the rest 70% of the raw materials were slowly and continuously placed on the running disc, and the water was still slowly sprayed on the dried materials surfaces. This process lasted 20 min until no new aggregates were produced, and then the produced aggregates were collected. The production efficiency of the aggregates is calculated as follows:

$$\text{Production efficiency} = \frac{W_{certain\ \ size}}{W_{total\ \ size}} \times 100\% \quad (1)$$

Where $W_{certain\ size}$ is the weight (g) of the synthesized aggregates at a certain size and $W_{total\ size}$ is the total weight (g) of the synthesized aggregates of all sizes.

The obtained aggregates need to be sealed by plastic bags to harden and form for 24 h to avoid the loss of water evaporation. Finally, the aggregates were cured in an environment (21 ℃ and 98% relative humidity) for 28 days in order to get the necessary strength. In addition, high humidity was chosen as the curing condition in this experiment considering the report by Shafigh et al. [41], which concluded that moist curing could reduce the decrease of strength in oil pal shell-blended fly ash lightweight concrete than air curing.

2.4. Testing methods

2.4.1. Physical properties

Prior to the below characterizations, the aggregates were put into the oven at 105 ℃ for 24 h. The loose-filled bulk density was tested according to EN 1097–3. The bulk density (ρ_b) of a single aggregate was calculated and obtained via the cross-section image processed by ImageJ software. The description is detailed in the literature [42,43]. The apparent density (ρ_a) and true density (ρ_t) are measured using a helium pycnometer performed on the aggregate and the milled powder, respectively. The closed porosity ($\varnothing_{closed}$) of the aggregate was calculated following:

$$\varnothing_{closed} = \rho_b * \left(\frac{1}{\rho_a} - \frac{1}{\rho_t}\right) \times 100\% \quad (2)$$

The total porosity ($\varnothing_{total}$) of the aggregate was calculated as follows:

$$\varnothing_{total} = \left(1 - \frac{\rho_b}{\rho_t}\right) \times 100\% \quad (3)$$

The water content and water absorption test of SLWAs were determined following the ASTM C-127. To evaluate the shape of SLWAs, the flattening coefficient p, was as follows:

$$p = \frac{\mathrm{e(thickness)}}{\mathrm{I(width)}} \quad (4)$$

The elongation coefficient q, was as follows:

$$q = \frac{\mathrm{I(width)}}{\mathrm{L(length)}} \quad (5)$$

For each granular fraction, 20 aggregates were measured based on the literature [44]. According to Zingg's classification method [45], the shape of aggregates is categorized into four types: disk, spherical, blade, and rod (Fig. 3).

Furthermore, the sphericity (Φ) of aggregates is calculated following Wadell's formula, as below.

$$\Phi = \sqrt[3]{q^2 \times p} \quad (6)$$

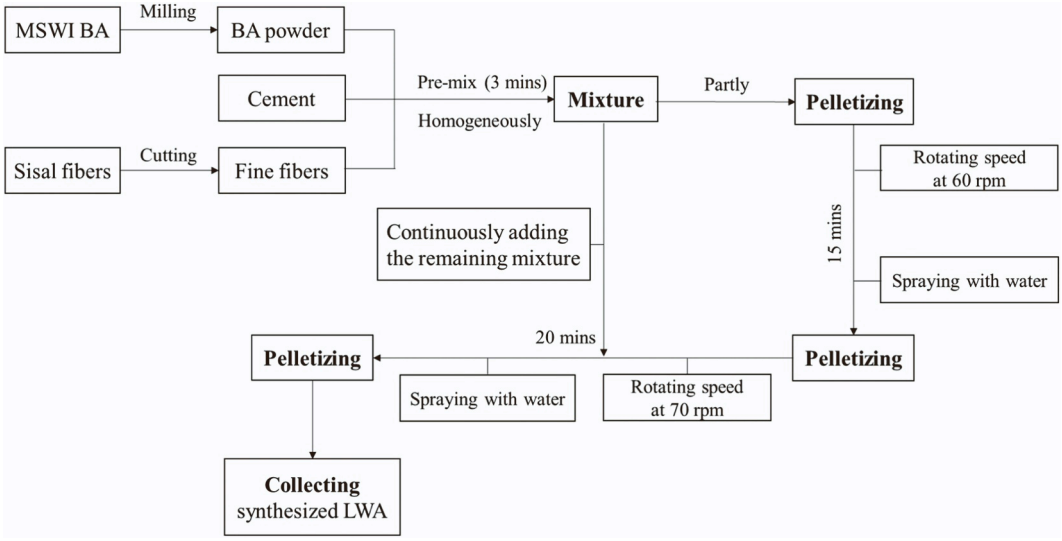

Fig. 2. The manufacturing process of SLWAs.

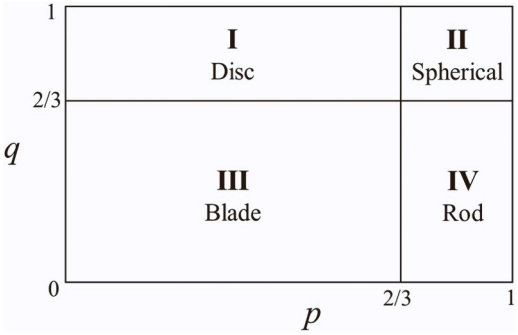

Fig. 3. Zingg's classification of particle shape.

2.4.2. Mechanical performance

The crushing strength of a single synthesized aggregate in this study is obtained by adapting a modeling calculation proposed by [46]. The test was conducted using the EZ 20 Lloyd Instrument machine with a 30 kN loading cell, accurate to 1/1000th of the load cell capacity, at a loading speed of 0.8 mm/min until it is broken, as shown in Fig. 4.

20 pellets in each subgroup were statistically tested and the results of peak force were recorded. According to the literature [46], the crushing strength was calculated following the relation.

$$\sigma_{crushing} = \frac{2.8P}{\pi d^2} \tag{7}$$

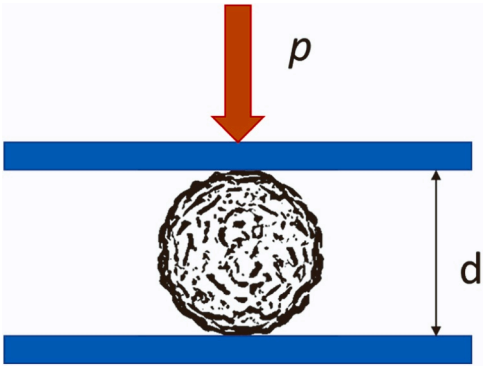

Fig. 4. Crushing strength of individual pellet.

Where σ is the crushing strength of individual aggregate (MPa), *P* is the peak force (N), and d (mm) is the distance between the points of loading.

The above (7) was built on the hypothesis that fracture along the middle part of the test samples. As can be seen from Fig. 5, the crack propagated along the middle axis, which proves that it is reasonable to employ this modeling formula performed on the synthesized aggregates in this experiment.

2.4.3. Microscopic properties

To analyze the microscopic performance difference of SLWAs with or without sisal fibers, the cross-section microstructure of crushed aggregates was characterized with a Zeiss optical microscope and scanning electron microscopy (SEM, Phenom ProX, PhenomWorld). The surface roughness of the SLWAs was quantified by phenom 3D roughness reconstruction software. The field of view is between 10 μm and 2 mm. Ra (average roughness) is automatically calculated and obtained. In addition, to better understand the underlying effect of the hydration kinetic of aggregates on strength development, the isothermal calorimeter (TAM air, Thermometric) is employed to study the hydration reaction of synthesizing the aggregates. However, the mixtures for producing aggregations are difficult to disperse due to the low water/solid (MSWI BA and cement) ratio. To address this problem, the water/solid ratio is increased to 0.5 to prepare the samples for calorimeter measurement. Various ratios of MSWI BA, cement, and/or SF were blended in glass bottles. Following 3 min of manual shaking, water was added to the glass bottles, and mixing was performed using a glass rod. The mixed samples were then sealed and loaded into an isothermal calorimeter that had reached thermal equilibrium at 20 ℃. After nearly 2 weeks, the test was stopped, and the samples were removed. The obtained data were subsequently analyzed and compared.

2.4.4. Leaching evaluation of SLWAs

The environmental impact of the investigated SLWAs is evaluated by the leaching test according to the Dutch legislative standard NEN 7383, 2003. The crushed aggregates after a single compressive strength test are sized below 4 mm before the test. The crushed aggregates were placed into a sealed plastic bottle (L/S = 10) and shaken at 200 rpm for 24 h. After that, the leachates were filtered through the 0.2-um filter to prepare solutions for the heavy metal ions test (Inductively coupled plasma atomic emission spectrometry, ICP-AES) and anion test (Ion chromatography, IC).

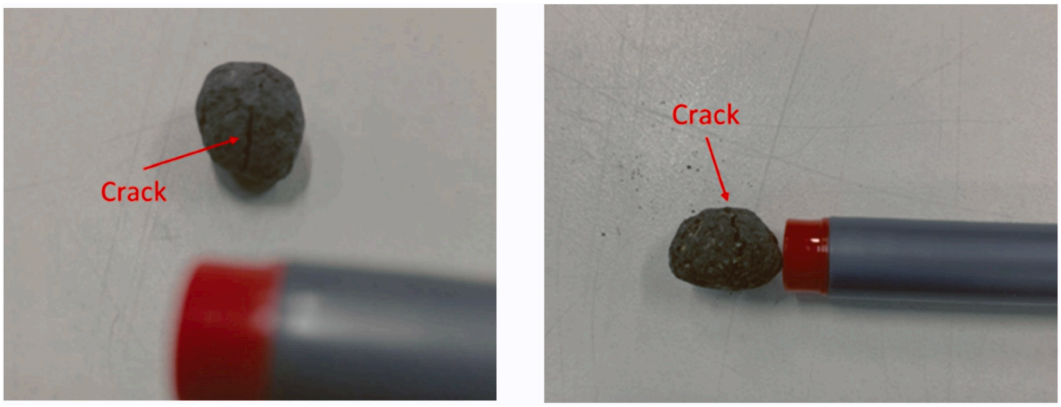

Fig. 5. Crack propagation of typical aggregates without SF(a) and with SF (b).

2.4.5. Environmental and Economic Evaluation

According to the literature [47], [48], [49], the approach of life cycle assessment (LCA) has been employed to evaluate the environmental impact of lightweight aggregates synthesized by solid waste. In this work, the cradle-to-gate method within the LCA was employed to evaluate the environmental impact of synthesized MSWI BA-based aggregates. The impact assessment was carried out using the ReCiPe midpoint (H) method. The LCA approach includes the following steps: 1) goal and scope definition: the goal of this LCA was to evaluate and compare the GHG emissions resulting from producing MSWI BA-based aggregates with/without sisal fibers and the production of 1 kg aggregates regarded as a functional unit; 2) Life cycle Inventory (LCI) analysis: Input unit sources in the LCA are listed in Table 4; 3) Life cycle impact assessment; 4) Life cycle interpretation [50]. LCA modeling was performed using SimaPro software (version 9.0.0.48) within the LCA to assess the GHG emissions.

Additionally, cost calculation serves as another crucial criterion to evaluate the practical applicability of the synthesized MSWI BA-based aggregates. In this study, the cost assessment currently considers laboratory-scale production. Raw materials prices and processing costs including transport and electricity fees are derived from the average prices in the Netherlands or the Europen area. Detailed information is provided in the corresponding section (Section 3.5.2).

3. Results and discussion

3.1. Physical properties

In this study, the aggregates with different replacement substitutes of MSWI BA were produced and the obtained production efficiency results are illustrated in Fig. 6. In general, synthesized coarse aggregates with 4 mm more (4–8 mm and >8 mm) account for the major percentage of produced aggregates. Therefore, considering the effective utilizing ratio of aggregates, coarse aggregates are chosen more than 4 mm in diameter size as the research objectives in this study. When SF is incorporated, the

Table 4
Source of unit process.

Type of Input data	Source
Cement	Ecoinvent 3 database, Cement, Portland {Europe without Switzerland} production
MSWI bottom ash	Ecoinvent 3 database, MSWI BA built based on the pretreated process in this study
Sisal fibers	Ecoinvent 3 database, jute modified
Water	Ecoinvent 3 database, water, the Netherlands
Electricity	Ecoinvent 3 database, natural gas, conventional power plant, NL
Transportation	Ecoinvent 3 database, lorry 16-32 metric tons, EURO5.

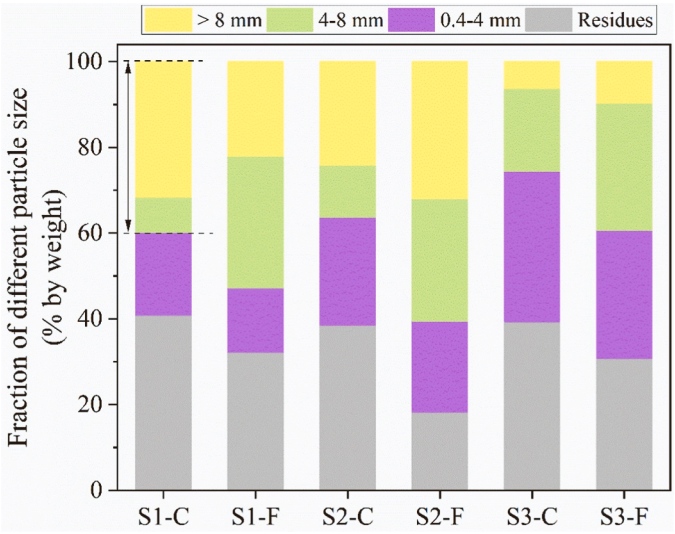

Fig. 6. Production efficiency of SLWA (equivalent diameter >4 mm) under different proportions.

production efficiency of coarse aggregates synthesized is obviously increased. In particular, the fraction of coarse aggregates in the S2-F is 60.54%, with the highest increment of 66.5% compared to the control S2-C. This indicates that SF can provide a bond effect in mixed powder (cement powder and MSWI BA powder) in the preparation process. According to the literature [51,52], cement powder and MSWI BA powder have positive charges, leading to the appearance of electrostatic repulsion forces. That means such forces would be set off to some extent the driving force produced from the hydrophilic characteristics of powders. Whereas, sisal fiber with both hydrophilic characteristics and negative charges [53] can not only take water absorption force to bind inorganic powder but also attract these negative-charged powder agglomerations to form aggregates. Furthermore, when cement replacement with MSWI BA increases, the production efficiency of the coarse aggregates without fiber incorporated generally decreases. This is in accordance with the previous study. However, it was noticed that sisal fibers incorporated have the best effect on production efficiency when the proportion of MSWI BA increases to 70 wt%. This could be due to the fact that when the amount of MSWI BA is lower, the water is easily absorbed by a higher proportion of cement, which leads to less bonding effect provided by sisal fibers due to their lower wetting surfaces. On the other hand, when the amount of MSWI BA exceeds 70 wt%, the cement binder is insufficient for the system, resulting in synthesized aggregate powder being prone to loosening and finally reducing the production efficiency of aggregations. Therefore, considering the efficient

production, the 70 wt% MSWI BA with sisal fibers is the optimum design ratio in this study.

Shape characteristics and physical properties of aggregates are significant parameters for assessing synthesized lightweight aggregates. Table 5 shows the morphological and physical properties of all studied aggregates. In terms of morphological performances, three main parameters: flakiness ratio, elongation ratio, and sphericity are focused on. According to Zingg's classification, three groups are categorized as spherical (flakiness ratio $>$ 2/3., elongation $>$ 2/3). Meanwhile, the shape of aggregates in the S2 group is the nearest closest to the spheric, with the highest levels of sphericity (0.87). The reason for this is unclear but it is possibly related to the design ratio of S2. The resulting early strength can effectively be resistant to impact force in the course of pelletizing. Besides, such a spherical shape can improve workability and affect the stress concentration of corresponding LWA concrete under loading [54]. The results of surface roughness show that sisal fiber incorporation can increase the roughness degree of synthesized aggregates, which can improve the interface property of concrete in the future. Among all the MSWI BA replacement groups, the S2-C and S2-F in the S2 group have the most significant difference in surface roughness as can be seen in Table 5. The corresponding surface roughness profiles are depicted in Fig. 7.

In terms of water absorption, the data presents that SLWAs produced with S1-F, S2-F, and S3-F perform relatively higher compared to those without SF. This could be related to their microstructure changes due to the SF incorporation. Commonly, plant fibers have a hollow lumen structure, which is prone to absorb water via capillary force [25]. The detailed explanation is further discussed in the following sections. In addition, the loose bulk density of the aggregates is also shown in Table 5. This shows that the loose bulk density of all aggregate samples is in the range of 633.52–882.81 kg/m^3, which meets the density requirement (between 500 and 1200 kg/m^3) of LWAs according to UNI EN 13055–1:2005 standard. High replacement levels result in a decreased density of the aggregates, which is attributed to the binder content decreases [7]. Whereas, at each substitution level, the SF added can increase the loose bulk density of synthesized aggregates. In fact, there are certain macro and micro pores generation resulting from hydrogen gas release of the metallic aluminum contained MSWI BA, reacted with alkali [11]. SF incorporation can fill the pore spaces and increase the density to some extent. This will be further proved by the following cross-section observation with SEM. Meanwhile, this analysis implied the pore structures are likely to affect the mechanical performance of the SLWAs. To under the effect, the strength of single aggregates is studied in the subsequent section.

3.2. Strength of individual aggregate

The strength property of synthesized aggregates is likely to depend on two fundamental aspects. First, the low-activity MSWI BA replacement can negatively influence the hydration kinetics of the binder cement, thus leading to a reduction of strength [55]. Second, the mixture of MSWI BA and cement results in pores generation from metallic aluminum reacting in the alkali environment, seriously hindering the development of structural strength [9,55].

The strength results of individual aggregate with 4–15 mm are presented in Fig. 8. The data of the individual aggregate strengths are relatively dispersed since this strength test would be affected by the chosen single aggregate [40]. Therefore, to more clearly exhibit the correlation between the strength properties and the aggregate size, we fitted these dispersed data to analyze and compare. According to the data of the peak force and particle size (Fig. 8(a, b, and c)), the peak force statistically increases with the rising equivalent diameter of individual SLWA regardless of with/without SF incorporation. This trend is well in agreement with the reports of [38,56]. However, as the replacement level with MSWI BA increases, the average peak forces of the aggregates gradually decrease. Increased MSWI BA content not only reduces the potential degree of pozzolanic reaction within the CEM-MSWI BA system [36,37] but also generates more pore spaces due to the increase in the metallic aluminum content [57,58]. The combination of both factors leads to serious negative effects on the load force. This can be in line with the loose density measurement. According to the data regression analysis, the addition of SF enhances the peak force of individual particles, which is highly related to the filling role of plant fiber. Here, the filler role of SF in the CEM-MSWI BA system is thought a combination of both a physically filling effect and a seeding effect (hetero nucleation and growth). The deep analysis will be discussed in the following sections. In addition to filling the pores, incorporated SF has high stiffness that helps in resistance to compression force. It has to be noted from the fitting non-linear curves that the strengthening effect of SF becomes more significant when the equivalent diameter increases. This could depend on the MSWI BA content of the individual aggregate.

The correlations between crushing strength and pellet diameter size were calculated and obtained in Fig. 8(a′, b′, and c′). The crushing strength of SLWAs decreases with the increase of the aggregate size, which is consistent with the discovery of Liu et al.[38].investigated the single-particle compression test of artificial MSWI BA-based aggregates and found the peak force increases with the increase of the single-aggregate size. In contrast, the relation between the crushing strength and the aggregate size is a positive correlation for the SF addition. In particular, in the S2 group (70% replacement), SF addition exhibited the most significant strengthening effect on the SLWAs. In general, plant fiber added to the cementitious matrix can improve the flexural strength of the composites by resisting cracking destruction.

To deeply understand the effect of the SF addition on the CEM-MSWI BA system, we analyze the hydration kinetics of the mixtures and microstructures of SLWAs in subsequent sections.

3.3. Microscopic properties analysis

3.3.1. Calorimetry

The calorimetry results are shown in Fig. 9. It can be seen from Fig. 9 (a) that the heat flow rate is quite low, which is mainly due to the major content of low-active MSWI BA incorporation. In addition, several peaks derived from one curve appeared at different hydration times, as shown in Fig. 9(b) and (c). It is unclear but it is probably related to the accelerating/retarding effect of some element components of MSWI BA. Kumar et al. [59] concluded that some heavy metal elements like Cu and Fe can retard cement hydration while the others like Pb and Br appear to

Table 5
Geometrical characteristics and physical properties of synthesized coarse aggregates under different proportion.

		S1		S2		S3	
		C	F	C	F	C	F
Shape parameters	Flakiness ratio	0.89	0.86	0.92	0.90	0.85	0.86
	Elongation ratio	0.88	0.83	0.86	0.86	0.81	0.86
	Sphericity	0.87	0.84	0.87	0.87	0.82	0.86
Surface roughness (Ra, μm)		2.92	4.07	3.20	5.09	2.91	3.18
Water absorption (%)		22.81	28.17	24.17	29.55	32.23	36.23
Loose-filled bulk density (kg/m^3)		720.92	882.81	675.50	695.42	633.52	652.61

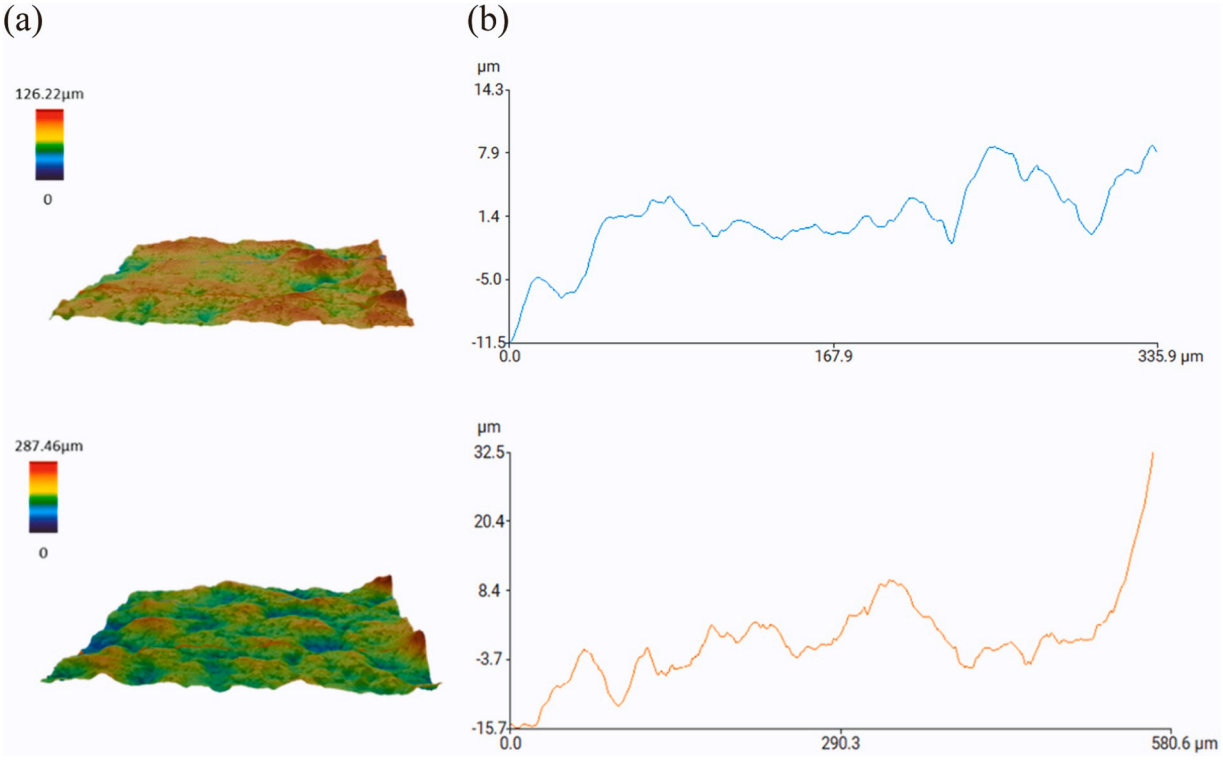

Fig. 7. Surface roughness appearances and corresponding type lines of coarse aggregates: S2-C (a) and S2-F (b).

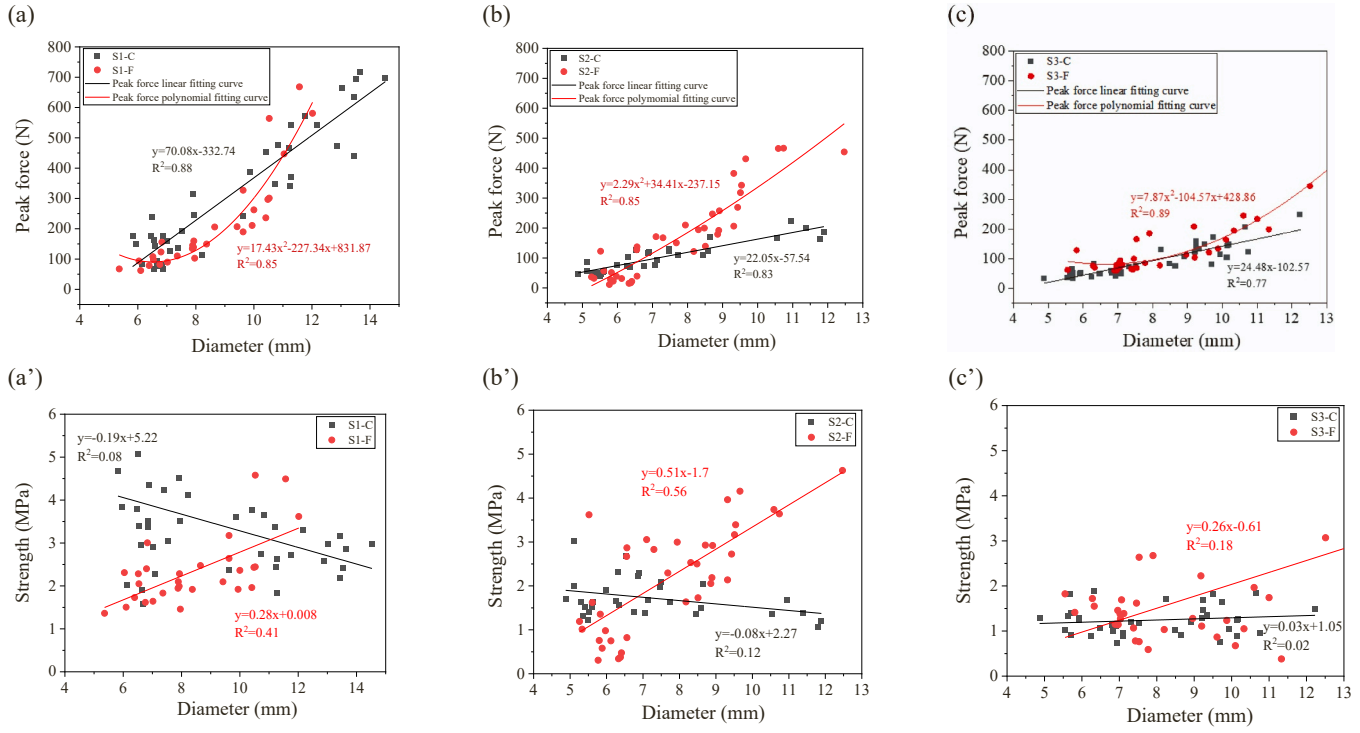

Fig. 8. Relationships between SLWA size and peak force (a, b, and c), and strength (a′, b′ and c′).

accelerate cement hydration. Interestingly, the total heat release of the mixture with SF exceeds that of the mixture without SF at all substitution levels as the hydration time increases. There are two potential reasons for this phenomenon, one is likely because of the internal curing role of SF [60,61]. SF, due to the hollow lumen structure, absorbs the alkali pore solution containing OH- inside its structure in the initial hydration period. However, at the later period of hydration time, as the moisture of the system is lost, the solution absorbed by SF is slowly released. At this time, the hydroxyl ion in the alkali pore solution can continue to dissolve the metallic aluminum from MSWI BA, forming alumina tetrahedral and finally participating in the system cementitious reaction. These exothermic processes of dissolution and reaction further

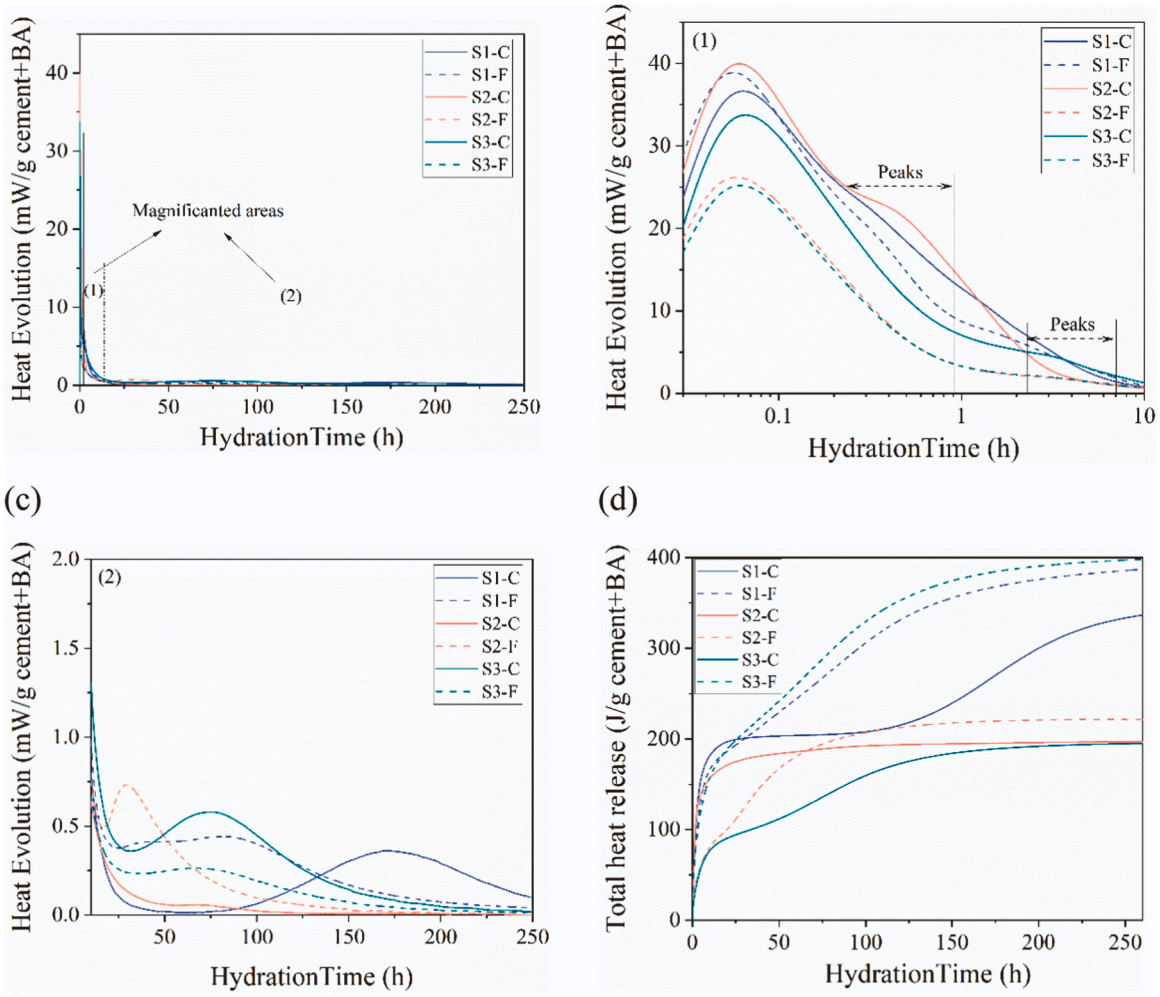

Fig. 9. Heat evolution: (a) entire-period curves (b) the curve in the initial 10 h and (c) the curves between 10 and 250 h, and total heat release (d) normalized to the solid mass (cement plus MSWI BA).

increase the total heat release. The other is closely related to the extra hetero nucleation sites due to the presence of the SF, which can accelerate the system hydration reaction. The deep mechanism explanation will be discussed in Section 3.4.

To clearly observe the influence of SF incorporation on the system hydration parameters, the correlation between hydration parameters and SF at the different replacement levels of MSWI BA was depicted in Fig. 10. The SF incorporation is positively correlated with the time at the maximum heat flow (final setting time), as shown in Fig. 10(a). The time advance suggests that fiber incorporation can accelerate the hydration

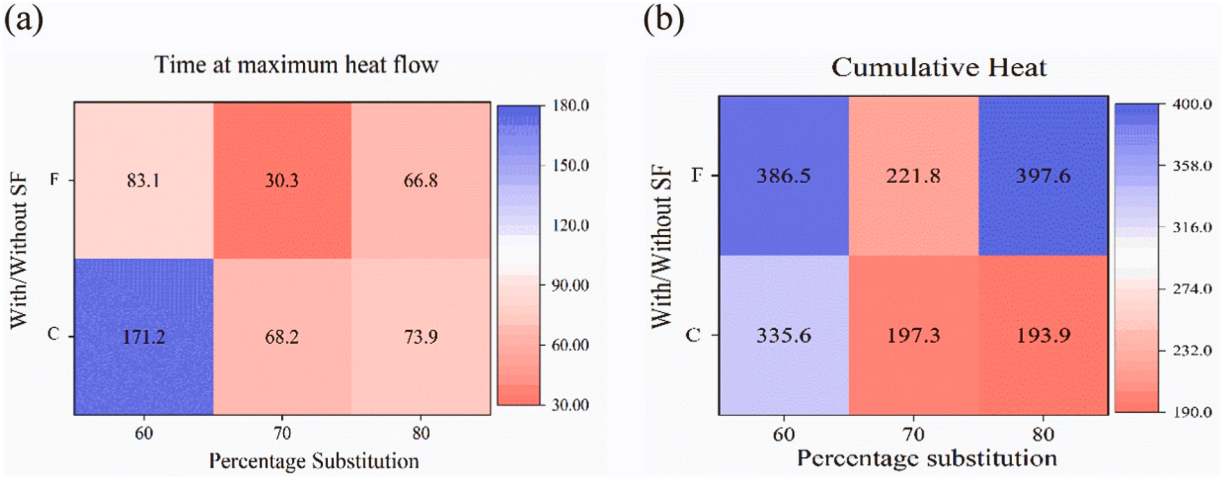

Fig. 10. Heat map of correlation between SF contained at the different substitution of MSWI BA and hydration parameters: (a) final setting time and (b) cumulative heat of SLWAs.

reaction via increased hetero nucleation sites, which is in line with the above analysis of total heat release. The cumulative heat result (Fig. 10 (b)) indicated that SF added can significantly promote the hydration kinetics of the CEM-BA system. In particular, the SF incorporation under the 70% substitution level achieves the highest cumulative heat, indicating the added SF plays the best optimal role in this substituted system.

3.3.2. Microstructure and pore structure

The optical microscope and SEM images of S2-C and S2-F are shown in Fig. 11. According to the optical images, the synthesized aggregates without fibers have many micropores and some small pores, whereas only several small pores were observed in the aggregates with fibers. Meanwhile, the fiber and the cementitious matrix are well-bonded. The reason for this phenomenon could be due to the hydroxyl and carbonyl groups on the fiber surfaces, which can promote the nucleation and growth of the calcium silicate hydrate C-S-H gel and chemical bonding with cementitious matrix [62,63].

The SEM images of samples S2-C and S2-F are depicted in Fig. 11 (b) and (d). It can be observed that both the amount and size of pores in S2-C are much more than those of sample S2-F. This indicates that the sisal fiber incorporation can densify the aggregates, which is attributed to the pore filling and accelerated hydration through extra hetero-nucleation sites provided.

To quantify the proportion of pore spaces, the porosity of aggregates under different replacements with/without fibers is measured, as shown in Fig. 12. The total porosities of the aggregate samples (S1-S3) generally increase as the replacement level with BA increases. This is consistent with the strength behaviors of the aggregates at different replacement levels. However, in terms of closed porosity, S2-F at a 70% replacement level, displays the lowest (1.97%). There are possibly two reasons for this. One is related to the closed pore size, which matches the size of the fiber diameter. This is well confirmed by the above optical microscope observation. Another possible reason is when the replacement level is from 60% to 70%, the increased BA tends to lead to increased pore amount and expanded pore size, which means many open pore amounts are generated and closed pore amounts are relatively reduced. As it continues to increase to 80%, the expanding degree of the pore size and the increase of the pore amount gets relatively weak due to much less cement incorporation. Therefore, this is why the increasing trend of total porosity trend is kept, not presenting the same turning point as the closed porosity.

3.3.3. Leaching behavior

Considering some hazardous substances contained in MSWI BA, it is necessary to assess the potential environmental impact of the synthesized aggregates in this study. The leaching test was performed on the leachate from the SLWAs, focusing on the concentration of the type of harmful anions (chloride and sulphate) and certain hazardous heavy metal cations. The leaching data is shown in Table 6.

It can be seen from the comparison of the leaching data with the legislation limitation values, that the values for the SLWAs are far below the legislation limitation of building materials applied in insulation facilities. This suggests that the synthesized aggregates can be applied in certain construction facilities by enclosing them with an outer layer such as in the liquid-tight paving application. Compared to the limit values of unmolded materials, the leaching emissions of partially harmful elements in the SLWAs have not yet met the legislation criteria, but it is not difficult to estimate that when the aggregates used as lightweight concrete, the leaching emissions of the resulting composites will be considerably reduced or even below the limit values.

The results show that the leaching values of tested hazardous element ions are significantly decreased after ground MSWI BA is processed into the SLWAs. This is likely to be the fact that the hydration products like C-S-H gel and ettringite generated from the reaction of cement and MSWI BA immobilize these harmful ions, thus reducing their

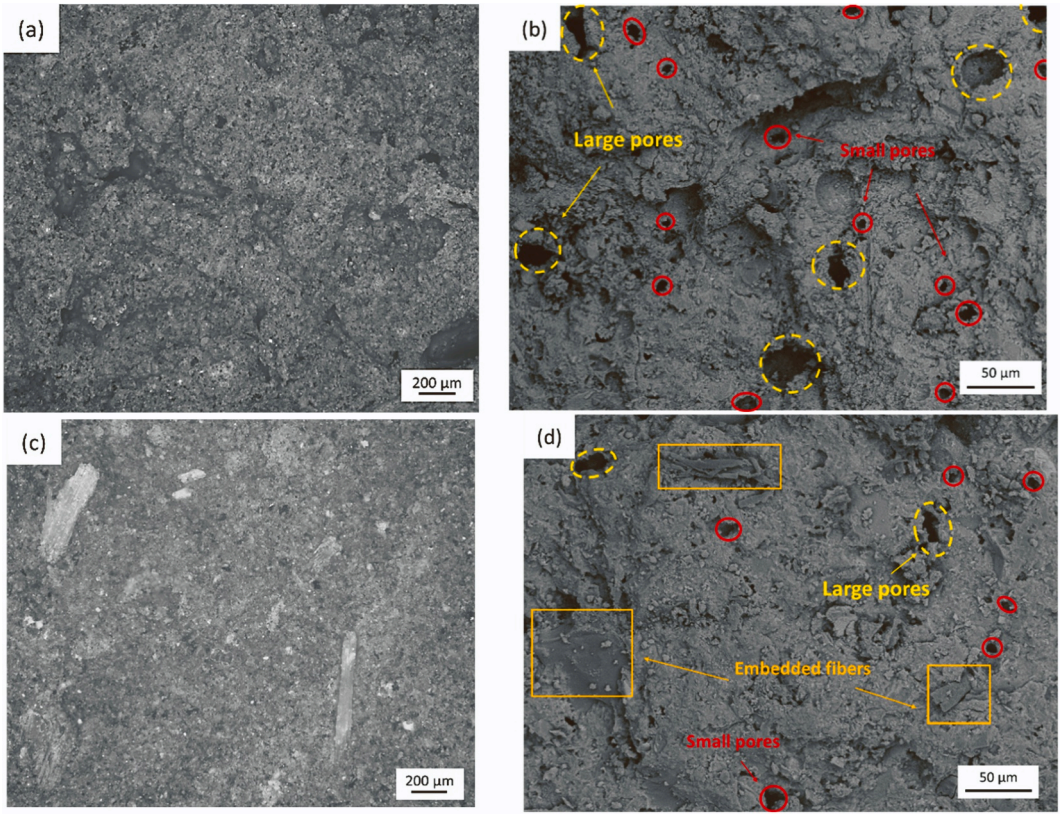

Fig. 11. The optical microscope cross-section images of S2-C (a) and S2-F (c);the SEM images of S2-C (b) and S2-F (d).

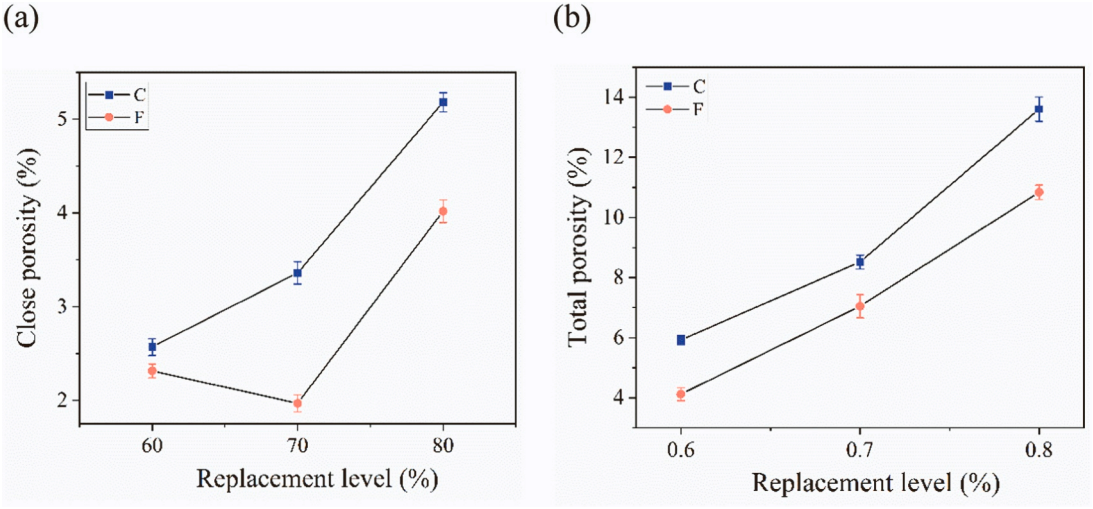

Fig. 12. Porosites of the synthesized aggregates: closed porosity (a) and total porosity (b).

Table 6
Leaching of chloride and sulphate, and heavy metal cations present in the leachates for raw materials (cement and ground MSWI BA) and SLWAs. LL is the legislation limit of building materials in the Netherlands [66].

Leaching value /mg/kg d.m. Samples	Chloride	Sulphate	Ba	Cr	Cu	Mo	Zn
Ground MSWI BA	8682	13865	0.98	0.4	7.01	3.77	0.84
CEM I 52.5 R[6]	322	52	30000	0.5	< 0.01	0.2	0.04
S1-C	2410	75.4	13.32	0.35	3.46	0.81	0.36
S1-F	2260	207	9.45	0.26	3.21	0.67	0.22
S2-C	3320	429	3.16	1.19	4.91	2.43	0.2
S2-F	2710	878	2.1	0.82	4.77	2.27	0.18
S3-C	4800	874	2.25	1.01	7.28	3.04	0.16
S3-F	4570	757	1.62	0.78	7.06	2.82	0.13
LL[a]	616	1730	22	0.63	0.9	1	4.5
LL[b]	8800	20000	100	7	10	15	14

mg/kg d.m. refers to the mg per kg of dry matter
LL[a] refers to the legislation limit of the building materials that have not been molded.
LL[b] refers to the legislation limit of the building materials that only can be applied in insulating facilities.

release [64]. As regards the comparison of the experimental aggregates with reference aggregates, the leaching values of the aggregates reinforced with SF can effectively decrease the release of contaminated ions, except for the sulphate anions. The reason for this unusual phenomenon is unclear but is possibly related to the polysaccharides of sisal fibers. This could capture the Ca^{2+} from gypsum, leading to the potential release of sulphate [65].

Overall, after ground MSWI BA is processed into SLWAs, their leaching values of hazardous ions can satisfy the environmental-friendly requirement.

3.4. Further mechanism analysis

It is well known that the water-soluble extractives and polysaccharides of plant fiber retard the normal setting and then influence the strength development of the fiber/cement composites [67,68]. However, in this study, plant fiber added in the CEM-MSWI BA system comprehensively exhibits a positive role in the strength property of the synthesized aggregates, although the retarder effect also possibly exists. To better understand the underlying positive effects of plant fiber in the CEM-MSWI BA matrix, it is important to familiarize the chemical compositions of MSWI BA and its performance within an alkali cement environment. Unlike common supplementary cementitious materials (SCMs), MSWI BA contains a relatively higher amount of metallic aluminum, which readily reacts with alkali and then releases hydrogen gas. This release leads to pore generation, which can detriment the ultimate strength of the resulting CEM-MSWI BA composites [58]. To address it, SF was incorporated into the CEM-MSWI BA matrix for the production of lightweight aggregates.

Based on the characterization and analysis conducted in this study, two mechanisms of SF reinforcement are proposed: the filling effect and the seeding effect, as illustrated in Fig. 13. For the former, plant fiber incorporation can physically fill the pores produced from the reaction of MSWI BA in the cement system. For the latter, plant fiber can act as seeds, providing additional nucleation sites for the growth of the hydration products such as portlandite and the calcium silicate hydrate C-S-H gel, as is shown in Fig. 14. Similar to the behavior reported in [69,70]. Meanwhile, plant fiber, as the internal curing agent [70], can more effectively and persistently induce the hetero nucleation and growth of inorganic matrix substances on its surface through the slow release of pore solution. and Ultimately, these two ways can help improve the overall density and compactness of the aggregates.

In terms of contaminant immobilization, plant fibers with hollow structure is prone to absorb wastewater containing heavy metal ions by the capillary force [71]. This suggests that when SF was incorporated into the MSWI BA-OPC system, the pore solution containing heavy metal cations from MSWI BA also could be absorbed into the inner structure of the fiber (Fig. 15). Sequently, the heavy metal cations absorbed will be well fixed the inner surface of the fibers due to the electrical attraction. It is known that plant fiber is negatively charged due to the existence of

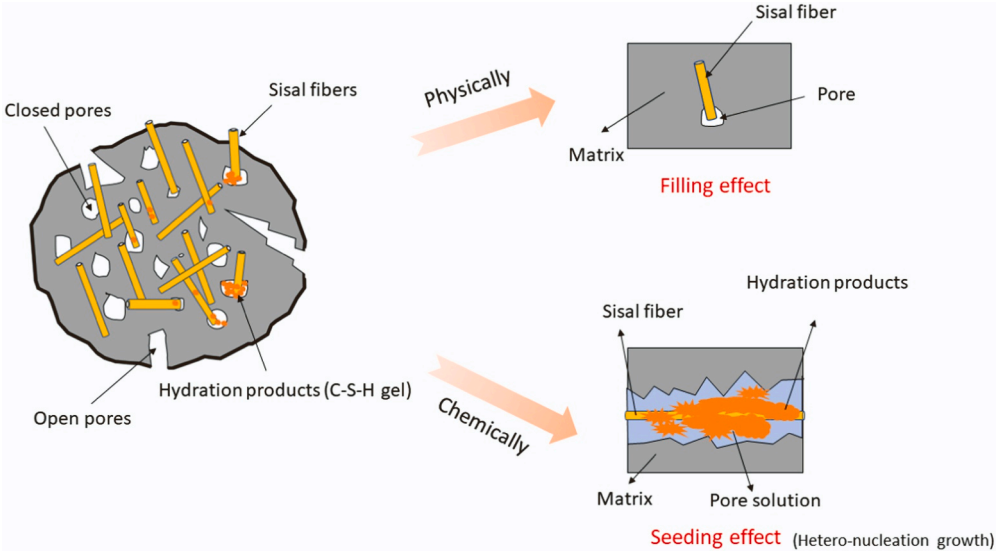

Fig. 13. Mechanism schematic in strength development of the SLWAs with SF.

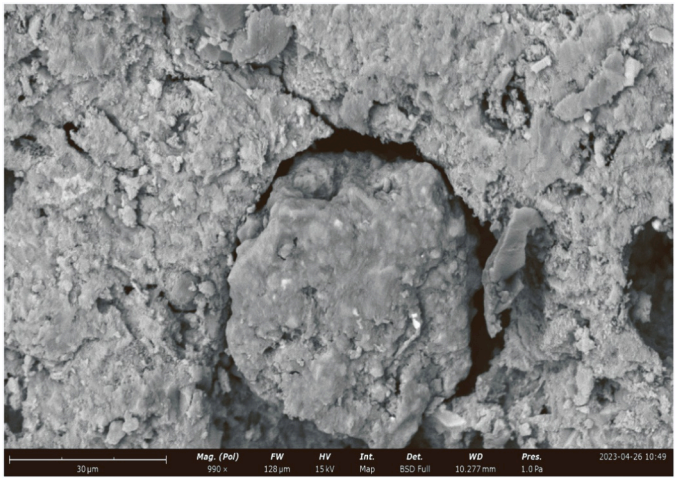

Fig. 14. A scanning electron micrograph (SEM) of the cross-section of S2-F.

some functional groups like carboxylic groups [29,72]. Also, it was reported that heavy metal elements are in the form of their cations distributed in MSWI BA [73]. That means it is probably theoretically possible for the heavy metal cations to be absorbed onto the inner surface of the fibers. Finally, The leaching data of the SLWAs confirmed the above hypothesis of the immobilization mechanism.

3.5. Environmental and economic evaluation

3.5.1. Environmental assessment

The greenhouse gas emission generated by the manufactured aggregates was evaluated as an indicator of environmental impact. To quantify the greenhouse gas emission of SLWAs, life cycle assessment (LCA) was employed in this study according to ISO 14040. Due to the fact that the MSWI BA is one waste substance, the energy consumption and greenhouse gas emissions generated by MSWI BA production are not considered in the following LCA calculation. The transportation distance for delivering raw materials was considered 200 km, (252 km is the longest straight line distance in the Netherlands, referring to [74]).

The global warming impact of SLWAs is shown in Fig. 16. It can be seen that the greenhouse gas emissions comprehensively continue to decrease as the replacement rate with MSWI bottom ash increases. In addition, SF incorporation can help reduce the global warming impact when the replacement level is the same. This is highly related to the enhanced production efficiency of the SLWAs due to the bridging effect of the fibers. For example, with the S2 group (70% replacement), the global warming impact of S2-F is significantly decreased by about 156 g CO_2 eq./kg (a decrease of 21%) in comparison with the S2-C. That means, S2-F is the best candidate among them considering the global warming impact, which has great potential for the sustainable building industry.

3.5.2. Cost evaluation

Bottom ash is a waste solid residue sourced from municipal waste burning. For the waste-to-energy plants, MSWI BA disposal requires additional costs like landfill tax [75]. Therefore, The MSWI BA can be obtained at zero cost for manufacturers. Sisal fibers used are the waste material from area cut palm, which is available for free. The cost data for the remaining materials and their corresponding processing are sourced from the Alibaba online website in the Netherlands region or the broader European area [76], as outlined in Table 7.

According to the data above in Table 7, the cost of synthesized aggregates at different substitutions with MSWI BA (Fig. 17). The cost data

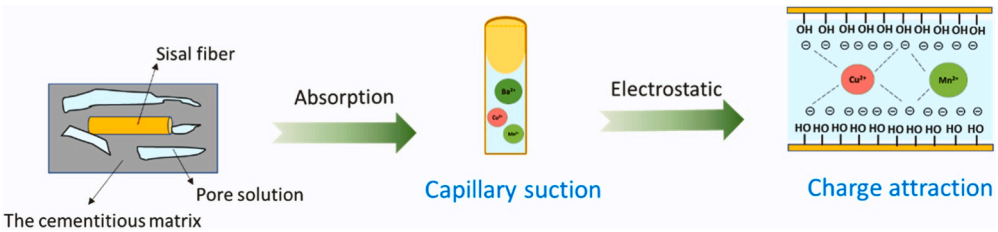

Fig. 15. Mechanism schematic in contaminant immobilization of the SLWAs with SF.

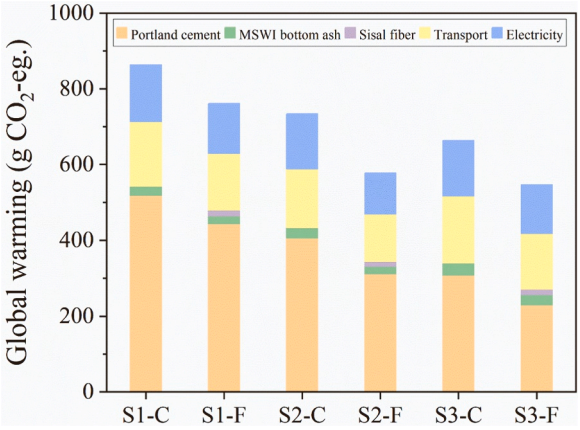

Fig. 16. Global warming impacts per 1 kg of aggregates preparation.

shows that as the substitution level increases, the cost of the SLWAs exhibits a decreased trend. This suggests that the dosage of MSWI BA used plays an important role in reduced cost. Comparing the S2 group and S3 group, the cost gaps of the SLWAs are smaller, which is attributed to the decreased production efficiency with increased MSWI BA. In addition, it is because of the production efficiency sisal fiber can promote, the aggregates reinforced with fiber generally lower cost advantages at the same replacement level. Expanded clay aggregates common commercial LWAs. The price is between €90/m^3 and €120/m^3, which averages far above the cost of the SLWA (both S2 and S3). That means, in the aspect of materials cost, such SLWA aggregates have the potential to be competitive. Finally, combined with the strength analysis above, the S2-F is the best candidate for the SLWAs production.

In conclusion, the studied SLWAs can not only be friendly to the environment in terms of the green housing gas emission and hazardous contaminant leaching but also have huge economic benefits in the lightweight aggregates market.

4. Conclusion

This comparative experiment aims to study the feasibility of the SF incorporation into synthesized MSWI BA aggregates in terms of strength improvement and contaminant leaching solidification. 2 wt% SF was added into the SLWAs with different replacement levels of MSWI BA. The impacts of SF on the physical characteristics, strength performance, microscopic properties, and sustainability of the produced aggregates were investigated. The following conclusions are drawn:

- The incorporation of SF can promote the production efficiency improvement of SLWAs by both hydrophilic nature and charge attraction of the fiber. The surface roughness extent of aggregates containing SF is obviously increased, which benefits the improved interface property of further concrete engineering.
- With increased MSWI BA content, the strength properties of SLWAs are reduced. However, the SF addition can considerably strengthen the strength performance of relatively large-diameter SLWAs, by improving the cement hydration kinetic (seeding effect) and reducing the porosity-filling effect. Especially, the SF shows the most remarkable strengthening effect of the SLWAs at the 70% replacement level of MSWI BA.
- The SF added into the aggregates can effectively absorb chloride anions and some harm heavy metal ions from BA. Combined with the cement solidification effect, the harmful ion leaching requirement of some building applications like insulated facilities can be satisfied.
- Through the greenhouse gas emission calculation, it is concluded that the SF incorporation can evidently reduce greenhouse gas emissions when the SLWAs are prepared, particularly the S2-F (a decrease of 23%) compared to S2-C. In addition, for the cost evaluation, the cost of SLWAs has been greatly decreased in comparison with the commercial expanded clay aggregates.

Table 7
The cost of materials and processing for the preparation of the SLWAs.

	Raw materials				Process	
	OPC	MSWI BA	Water	Waste sisal fiber	Electricity	Transport
$Price_{(approx.)}$	123 €/ton	-	1.6 €/m^3	-	0.32 €/kWh	0.348 €/tkm

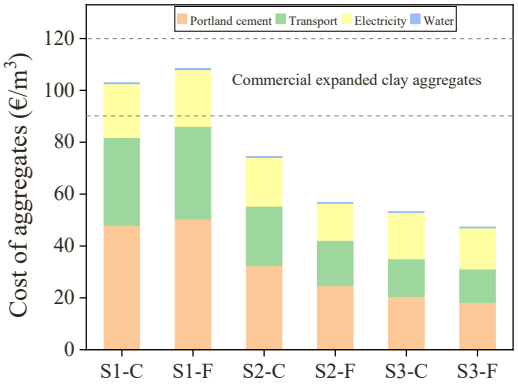

Fig. 17. The cost of the SLWAs under different replacement levels.

Therefore, our results support the feasibility of the SF as reinforcement for the cold-bonded granulation of MSWI BA. The SF incorporation not only enhances the strength properties of the SLWAs but also contributes to environmental benefits by reducing harmful ion leaching and greenhouse gas emissions. Furthermore, it is evaluated that the cost of SLWAs reinforced with SF is remarkably low, which has huge economic benefits.

CRediT authorship contribution statement

Song Helong: Writing – original draft, Methodology. **Gauvin Florent:** Writing – review & editing, Supervision. **Liu Tao:** Writing – review & editing, Methodology, Conceptualization. **Brouwers H.J.H.:** Writing – review & editing, Supervision.

Declaration of Competing Interest

The authors certify that they have no affiliations with or involvement in any organization or entity with any financial interest, or non-financial interest in the subject matter or materials discussed in this manuscript.

Data Availability

Data will be made available on request.

Acknowledgments

The work described in this study was supported by the China Scholarship Council (Grant No. 202006150020) and Eindhoven University of Technology. The authors thank (Heros, The Netherlands) for the supply of raw MSWI bottom ash. We also thank ENCI, the Netherlands for providing OPC for our experiments.

References

[1] M. Hasan, M. Rasul, M. Khan, N. Ashwath, M. Jahirul, Energy recovery from municipal solid waste using pyrolysis technology: a review on current status and developments, Renew. Sustain. Energy Rev. 145 (2021) 111073.

[2] D.M.Y. Maya, A.L.E. Sarmiento, C. Oliveira, E.S. Lora, R. Andrade, Gasification of municipal solid waste for power generation in Brazil, a review of available technologies and their environmental benefits, J. Chem. Chem. Eng. 10 (6) (2016) 249–255.

[3] L. Muchová, P. Rem, Metal content and recovery of MSWI bottom ash in Amsterdam, WIT Trans. Ecol. Environ. 92 (2006).

[4] A. Bourtsalas, Review of WTE ash utilization processes under development in northwest Europe, Doctoral student in Civil & Environmental Engineering, Imperial College, London (2013).

[5] L.A. Sormunen, A. Kalliainen, P. Kolisoja, R. Rantsi, Combining mineral fractions of recovered MSWI bottom ash: improvement for utilization in civil engineering structures, Waste Biomass-.-. Valoriz. 8 (2017) 1467–1478.

[6] E. Loginova, K. Schollbach, M. Proskurnin, H. Brouwers, Municipal solid waste incineration bottom ash fines: transformation into a minor additional constituent for cements, Resour., Conserv. Recycl. 166 (2021) 105354.

[7] R. Cioffi, F. Colangelo, F. Montagnaro, L. Santoro, Manufacture of artificial aggregate using MSWI bottom ash, Waste Manag. 31 (2) (2011) 281–288.

[8] P. Nielsen, M. Quaghebeur, B. Laenen, R. Kumps, P. Van Bommel, The use of MSWI-bottom ash as aggregate in concrete—limitations and possible solutions, WASCON (2009).

[9] U. Müller, K. Rübner, The microstructure of concrete made with municipal waste incinerator bottom ash as an aggregate component, Cem. Concr. Res. 36 (8) (2006) 1434–1443.

[10] P. Tang, W. Chen, D. Xuan, Y. Zuo, C.S. Poon, Investigation of cementitious properties of different constituents in municipal solid waste incineration bottom ash as supplementary cementitious materials, J. Clean. Prod. 258 (2020) 120675.

[11] S. Zhang, Z. Ghouleh, Z. He, L. Hu, Y. Shao, Use of municipal solid waste incineration bottom ash as a supplementary cementitious material in dry-cast concrete, Constr. Build. Mater. 266 (2021) 120890.

[12] F. Tajra, M.Abd Elrahman, D. Stephan, The production and properties of cold-bonded aggregate and its applications in concrete: a review, Constr. Build. Mater. 225 (2019) 29–43.

[13] J. Liu, Z. Li, W. Zhang, H. Jin, F. Xing, L. Tang, The impact of cold-bonded artificial lightweight aggregates produced by municipal solid waste incineration bottom ash (MSWIBA) replace natural aggregates on the mechanical, microscopic and environmental properties, durability of sustainable concrete, J. Clean. Prod. 337 (2022) 130479.

[14] G. Pecqueur, C. Crignon, B. Quénée, Behaviour of cement-treated MSWI bottom ash, Waste Manag. 21 (3) (2001) 229–233.

[15] L. Bertolini, M. Carsana, D. Cassago, A.Q. Curzio, M. Collepardi, MSWI ashes as mineral additions in concrete, Cem. Concr. Res. 34 (10) (2004) 1899–1906.

[16] V. Caprai, K. Schollbach, H. Brouwers, Influence of hydrothermal treatment on the mechanical and environmental performances of mortars including MSWI bottom ash, Waste Manag. 78 (2018) 639–648.

[17] K. Rubner, F. Haamkens, O. Linde, Use of municipal solid waste incinerator bottom ash as aggregate in concrete, Q. J. Eng. Geol. Hydrogeol. 41 (4) (2008) 459–464.

[18] D. Xuan, P. Tang, C.S. Poon, Limitations and quality upgrading techniques for utilization of MSW incineration bottom ash in engineering applications–A review, Constr. Build. Mater. 190 (2018) 1091–1102.

[19] X. Sun, Y. Yi, pH evolution during water washing of incineration bottom ash and its effect on removal of heavy metals, Waste Manag. 104 (2020) 213–219.

[20] C.H. Lam, A.W. Ip, J.P. Barford, G. McKay, Use of incineration MSW ash: a review, Sustainability 2 (7) (2010) 1943–1968.

[21] S. Arickx, T. Van Gerven, C. Vandecasteele, Accelerated carbonation for treatment of MSWI bottom ash, J. Hazard. Mater. 137 (1) (2006) 235–243.

[22] M.F. Bertos, X. Li, S. Simons, C. Hills, P. Carey, Investigation of accelerated carbonation for the stabilisation of MSW incinerator ashes and the sequestration of CO 2, Green. Chem. 6 (8) (2004) 428–436.

[23] Z. Giergiczny, A. Król, Immobilization of heavy metals (Pb, Cu, Cr, Zn, Cd, Mn) in the mineral additions containing concrete composites, J. Hazard. Mater. 160 (2-3) (2008) 247–255.

[24] M. Gougar, B. Scheetz, D. Roy, Ettringite and C□ S□ H Portland cement phases for waste ion immobilization: a review, Waste Manag. 16 (4) (1996) 295–303.

[25] A.R. de Azevedo, M.T. Marvila, B.A. Tayeh, D. Cecchin, A.C. Pereira, S. N. Monteiro, Technological performance of açaí natural fibre reinforced cement-based mortars, J. Build. Eng. 33 (2021) 101675.

[26] L. Gonzalez-Lopez, J. Claramunt, L. Haurie, H. Ventura, M. Ardanuy, Study of the fire and thermal behaviour of façade panels made of natural fibre-reinforced cement-based composites, Constr. Build. Mater. 302 (2021) 124195.

[27] H. Song, T. Liu, F. Gauvin, H. Brouwers, Improving the interface compatibility and mechanical performances of the cementitious composites by low-cost alkyl ketene dimer modified fibers, Constr. Build. Mater. 395 (2023) 132186.

[28] S. Anandaraj, S. Karthik, S. Sylesh, R. Kishor, K. Suresh, K.J. Prakash, K.D. Kannan, Experimental investigation on sugarcane bagasse fiber reinforced concrete using bottom ash as sand replacement, Mater. Today.: Proc. (2023).

[29] N.S.A. Rahman, M.F. Yhaya, B. Azahari, W.R. Ismail, Utilisation of natural cellulose fibres in wastewater treatment, Cellulose 25 (2018) 4887–4903.

[30] M. Bruno, M. Abis, K. Kuchta, F.-G. Simon, R. Grönholm, M. Hoppe, S. Fiore, Material flow, economic and environmental assessment of municipal solid waste incineration bottom ash recycling potential in Europe, J. Clean. Prod. 317 (2021) 128511.

[31] H. Li, H. Chu, Q. Wang, J. Tang, Feasibility of producing eco-friendly self-compacting mortar with municipal solid waste incineration bottom ash: a preliminary study, Case Stud. Constr. Mater. 19 (2023) e02309.

[32] Q. Wang, H. Chu, W. Shi, J. Jiang, F. Wang, Feasibility of preparing self-compacting mortar via municipal solid waste incineration bottom ash: an experimental study, Arch. Civ. Mech. Eng. 23 (4) (2023) 251.

[33] C. Shi, J. Li, S. Sun, H. Han, Research on pavement performance of cement-stabilized municipal solid waste incineration bottom ash base, Materials 15 (23) (2022) 8614.

[34] X. Zhu, B.-J. Kim, Q. Wang, Q. Wu, Recent advances in the sound insulation properties of bio-based materials, BioResources 9 (1) (2014) 1764-1786.

[35] P. Tang, M. Florea, P. Spiesz, H. Brouwers, Characteristics and application potential of municipal solid waste incineration (MSWI) bottom ashes from two waste-to-energy plants, Constr. Build. Mater. 83 (2015) 77–94.

[36] A. Mohanty, Ma Misra, G. Hinrichsen, Biofibres, biodegradable polymers and biocomposites: an overview, Macromol. Mater. Eng. 276 (1) (2000) 1–24.

[37] P. Tang, M. Florea, P. Spiesz, H. Brouwers, Application of thermally activated municipal solid waste incineration (MSWI) bottom ash fines as binder substitute, Cem. Concr. Compos. 70 (2016) 194–205.

[38] J. Liu, Z. Li, W. Zhang, H. Jin, F. Xing, L. Tang, The impact of cold-bonded artificial lightweight aggregates produced by municipal solid waste incineration bottom ash (MSWIBA) replace natural aggregates on the mechanical, microscopic and environmental properties, durability of sustainable concrete, J. Clean. Prod. 337 (2022).

[39] P. Tang, H. Brouwers, Integral recycling of municipal solid waste incineration (MSWI) bottom ash fines (0–2 mm) and industrial powder wastes by cold-bonding pelletization, Waste Manag. 62 (2017) 125–138.

[40] P. Tang, M. Florea, H. Brouwers, Employing cold bonded pelletization to produce lightweight aggregates from incineration fine bottom ash, J. Clean. Prod. 165 (2017) 1371–1384.

[41] P. Shafigh, U.J. Alengaram, H.B. Mahmud, M.Z. Jumaat, Engineering properties of oil palm shell lightweight concrete containing fly ash, Mater. Des. 49 (2013) 613–621.

[42] A.A. Agra, A. Nicolodi, B.D. Flores, I.V. Flores, G.L.R. da Silva, A.C.F. Vilela, E. Osório, Automated procedure for coke microstructural characterization in imagej software aiming industrial application, Fuel 304 (2021) 121374.

[43] E. Loginova, K. Schollbach, M. Proskurnin, H. Brouwers, Mechanical performance and microstructural properties of cement mortars containing MSWI BA as a minor additional constituent, Case Stud. Constr. Mater. 18 (2023) e01701.

[44] W. Juimo, T. Cherradi, L. Abidi, L. Oliveira, Characterisation of natural pozzolan of" djoungo"(cameroon) as lightweight aggregate for ligtweight concrete, GEOMATE J. 11 (27) (2016) 2782–2789.

[45] W.C. Krumbein, Measurement and geological significance of shape and roundness of sedimentary particles, J. Sediment. Res. 11 (2) (1941) 64–72.

[46] Y. Hiramatsu, Y. Oka, Determination of the tensile strength of rock by a compression test of an irregular test piece, Int. J, Rock Mech. Min. Sci. Geomech. Abstr. (1966) 89–90.

[47] A. Petrillo, F. Colangelo, I. Farina, M. Travaglioni, C. Salzano, R. Cioffi, Multi-criteria analysis for Life Cycle Assessment and Life Cycle Costing of lightweight artificial aggregates from industrial waste by double-step cold bonding palletization, J. Clean. Prod. 351 (2022) 131395.

[48] X. Shang, J. Chang, J. Yang, X. Ke, Z. Duan, Life cycle sustainable assessment of natural vs artificial lightweight aggregates, J. Clean. Prod. 367 (2022) 133064.

[49] A.B. López-García, M. Uceda-Rodríguez, S. León-Gutiérrez, C.J. Cobo-Ceacero, J. M. Moreno-Maroto, Eco-efficient transformation of mineral wool wastes into lightweight aggregates at low firing temperature and associated environmental assessment, Constr. Build. Mater. 345 (2022) 128294.

[50] C. Ingrao, A.L. Giudice, C. Tricase, C. Mbohwa, R. Rana, The use of basalt aggregates in the production of concrete for the prefabrication industry: environmental impact assessment, interpretation and improvement, J. Clean. Prod. 75 (2014) 195–204.

[51] I. Tanaka, M. Koishi, K. Shinohara, A study on the process for formation of spherical cement through an examination of the changes of powder properties and electrical charges of the cement and its constituent materials during surface modification, Cem. Concr. Res. 32 (1) (2002) 57–64.

[52] S. Ahmad, R. Kothari, H.M. Singh, V. Tyagi, B. Singh, A. Sari, Experimental investigation of microalgal harvesting with low cost bottom ash: Influence of temperature and pH with zeta potential and thermodynamic function, Environ. Technol. Innov. 22 (2021) 101376.

[53] V.H. Vargas, R.R. Paveglio, Pd.S. Pauletto, N.P.G. Salau, L.G. Dotto, Sisal fiber as an alternative and cost-effective adsorbent for the removal of methylene blue and reactive black 5 dyes from aqueous solutions, Chem. Eng. Commun. 207 (4) (2020) 523–536.

[54] I. Zafar, K. Rashid, M. Ju, Synthesis and characterization of lightweight aggregates through geopolymerization and microwave irradiation curing, J. Build. Eng. 42 (2021) 102454.

[55] G. Huang, K. Yang, L. Chen, Z. Lu, Y. Sun, X. Zhang, Y. Feng, Y. Ji, Z. Xu, Use of pretreatment to prevent expansion and foaming in high-performance MSWI bottom ash alkali-activated mortars, Constr. Build. Mater. 245 (2020) 118471.

[56] E. Güneyisi, M. Gesoğlu, Ö. Pürsünlü, K. Mermerdaş, Durability aspect of concretes composed of cold bonded and sintered fly ash lightweight aggregates, Compos. Part B: Eng. 53 (2013) 258–266.

[57] X. Qiao, M. Tyrer, C.S. Poon, C. Cheeseman, Novel cementitious materials produced from incinerator bottom ash, Resour., Conserv. Recycl. 52 (3) (2008) 496–510.

[58] N.M. Alderete, A.M. Joseph, P. Van den Heede, S. Matthys, N. De Belie, Effective and sustainable use of municipal solid waste incineration bottom ash in concrete regarding strength and durability, Resour., Conserv. Recycl. 167 (2021).
[59] V. Kumar, N. Garg, The chemical and physical origin of incineration ash reactivity in cementitious systems, Resour., Conserv. Recycl. 177 (2022) 106009.
[60] A. Mezencevova, V. Garas, H. Nanko, K.E. Kurtis, Influence of thermomechanical pulp fiber compositions on internal curing of cementitious materials, J. Mater. Civ. Eng. 24 (8) (2012) 970–975.
[61] S. Kawashima, S.P. Shah, Early-age autogenous and drying shrinkage behavior of cellulose fiber-reinforced cementitious materials, Cem. Concr. Compos. 33 (2) (2011) 201–208.
[62] M. Dadkhah, J.-M. Tulliani, Damage management of concrete structures with engineered cementitious materials and natural fibers: a review of potential uses, Sustainability 14 (7) (2022) 3917.
[63] Y. Gao, L.-Q. Liu, S.-Z. Zu, K. Peng, D. Zhou, B.-H. Han, Z. Zhang, The effect of interlayer adhesion on the mechanical behaviors of macroscopic graphene oxide papers, ACS Nano 5 (3) (2011) 2134–2141.
[64] X.-G. Li, Y. Lv, B.-G. Ma, Q.-B. Chen, X.-B. Yin, S.-W. Jian, Utilization of municipal solid waste incineration bottom ash in blended cement, J. Clean. Prod. 32 (2012) 96–100.
[65] F. Zhao, K. Xu, H. Ren, L. Ding, J. Geng, Y. Zhang, Combined effects of organic matter and calcium on biofouling of nanofiltration membranes, J. Membr. Sci. 486 (2015) 177–188.
[66] S.Q. Decree, 2007. ⟨https://rwsenvironment.eu/subjects/soil/legislation-and/soil-quality-decree/⟩.
[67] L. Aggarwal, J. Singh, Effect of plant fibre extractives on properties of cement, Cem. Concr. Compos. 12 (2) (1990) 103–108.
[68] M.O. Eloget, Suitability of Sisal Juice Extract as a Retarder in Cement Concrete, JKUAT-COETEC, 2022.
[69] T.D. Duong, K.L. Nguyen, M. Hoang, Competitive sorption of Na+ and Ca2+ ions on unbleached kraft fibres—a kinetics and equilibrium study, J. Colloid Interface Sci. 301 (2) (2006) 446–451.
[70] P. Jongvisuttisun, J. Leisen, K.E. Kurtis, Key mechanisms controlling internal curing performance of natural fibers, Cem. Concr. Res. 107 (2018) 206–220.
[71] C.M. Futalan, A.E.S. Choi, H.G.O. Soriano, M.K.B. Cabacungan, J.C. Millare, Modification strategies of kapok fiber composites and its application in the adsorption of heavy metal ions and dyes from aqueous solutions: a systematic review, Int. J. Environ. Res. Public Health 19 (5) (2022) 2703.
[72] A. Bismarck, A.K. Mohanty, I. Aranberri-Askargorta, S. Czapla, M. Misra, G. Hinrichsen, J. Springer, Surface characterization of natural fibers; surface properties and the water up-take behavior of modified sisal and coir fibers, Green. Chem. 3 (2) (2001) 100–107.
[73] P. Piantone, F. Bodénan, L. Chatelet-Snidaro, Mineralogical study of secondary mineral phases from weathered MSWI bottom ash: implications for the modelling and trapping of heavy metals, Appl. Geochem. 19 (12) (2004) 1891–1904.
[74] WorldAtlas, Maps Of The Netherlands, 2021. https://www.worldatlas.com/maps/netherlands. (Accessed May 20, 2023.
[75] S. Zhang, Z. Ghouleh, Y. Shao, Green concrete made from MSWI residues derived eco-cement and bottom ash aggregates, Constr. Build. Mater. 297 (2021) 123818.
[76] Alibaba.com, https://www.alibaba.com/.